

Transmitter Side Beyond-Diagonal RIS for mmWave Integrated Sensing and Communications

Kexin Chen, Yijie Mao

School of Information Science and Technology, ShanghaiTech University, Shanghai 201210, China

Email: {chenkx2023, maoyj}@shanghaitech.edu.cn

Abstract—This work initiates the study of a beyond-diagonal reconfigurable intelligent surface (BD-RIS)-aided transmitter architecture for integrated sensing and communication (ISAC) in the millimeter-wave (mmWave) frequency band. Deploying BD-RIS at the transmitter side not only alleviates the need for extensive fully digital radio frequency (RF) chains but also enhances both communication and sensing performance. These benefits are facilitated by the additional design flexibility introduced by the fully-connected scattering matrix of BD-RIS. To achieve the aforementioned benefits, in this work, we propose an efficient two-stage algorithm to design the digital beamforming of the transmitter and the scattering matrix of the BD-RIS with the aim of jointly maximizing the sum rate for multiple communication users and minimizing the largest eigenvalue of the Cramér-Rao bound (CRB) matrix for multiple sensing targets. Numerical results show that the transmitter-side BD-RIS-aided mmWave ISAC outperforms the conventional diagonal-RIS-aided ones in both communication and sensing performance.

Index Terms—Integrated sensing and communication (ISAC), millimeter-wave (mmWave), beyond-diagonal reconfigurable intelligent surface (BD-RIS).

I. INTRODUCTION

Integrated sensing and communication (ISAC) has emerged as a critical enabler for next-generation wireless networks. This attributes to its potential for sharing the spectrum, hardware architectures, and signal processing modules between communication and sensing functionalities. Meanwhile, the incorporation of millimeter-wave (mmWave) technique opens the door to high data rates for communications and high-resolution capabilities for target sensing [1]. Therefore, mmWave holds great promise for ISAC systems. However, owing to the severe path loss caused by the short wavelength characteristics of mmWave, a large number of transmit antennas along with extensive use of fully digital radio frequency (RF) chains are normally required at the transmitter to achieve high beamforming gain, resulting in huge power consumption [2]. This calls for low-cost solutions for mmWave ISAC systems.

One promising solution for mmWave ISAC is utilizing the reconfigurable intelligent surfaces (RIS) to assist the transmission. RIS, composed of numerous passive elements, shows its capability to reconfigure the wireless propagation environment for communication and sensing functionalities in the mmWave band [3]–[5]. Moreover, RIS adjusts the phase of the incident

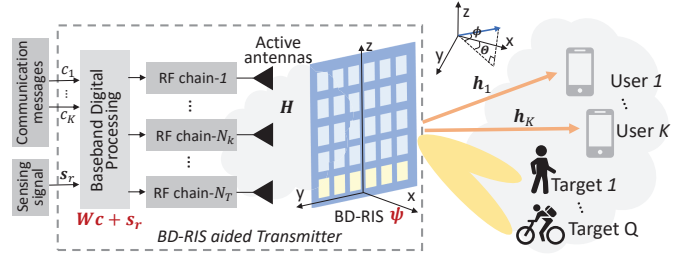


Fig. 1. The system model of BD-RIS-aided transmitter architecture for ISAC.

signals at an ultra-low power cost. It eliminates the need for extensive RF processing at the transmitter [2]. However, most of the existing studies on RIS-aided mmWave ISAC [3]–[5] primarily concentrate on the receiver-side RIS with more emphasis on the former benefit of RIS in propagation reconfiguration.

In addition, a revolutionary RIS architecture named beyond-diagonal RIS (BD-RIS) has been recently proposed [6], [7]. Different from conventional diagonal-RIS (D-RIS) where each element operates independently, in fully-connected BD-RIS [7], all elements are connected to each other. Recent studies [8], [9] have shown the superior performance gain of the receiver-side BD-RIS over conventional D-RIS in terms of both communication and sensing performance. However, the transmitter-side BD-RIS for ISAC system and its application in the mmWave frequency band has not been investigated yet.

Inspired by the transmitter-side RIS-aided communication network introduced in [2], [10], [11], in this work, we initiate the study of a transmitter-side BD-RIS-aided mmWave ISAC system. Specifically, we design the digital beamforming of the transmitter and the scattering matrix of the BD-RIS to jointly maximize the communication sum rate and minimize the largest eigenvalue of the sensing Cramér-Rao bound (CRB). An efficient two-stage optimization method is proposed, where the scattering matrix of the BD-RIS is obtained via the symmetric unitary projection, and the digital beamforming is optimized subsequently via the successive convex approximation (SCA) method. Numerical results demonstrate that BD-RIS-aided mmWave ISAC achieves a better communication and sensing trade-off compared to the conventional D-RIS-aided ones.

II. SYSTEM MODEL

As depicted in Fig. 1, we consider a mmWave ISAC system with a BD-RIS-aided transmitter simultaneously serving K

This work has been supported in part by the National Nature Science Foundation of China under Grant 62201347; and in part by Shanghai Sailing Program under Grant 22YF1428400. (Corresponding author: Yijie Mao)

single-antenna communication users and Q sensing targets indexed by $\mathcal{K} = \{1, \dots, K\}$ and $\mathcal{Q} = \{1, \dots, Q\}$, respectively. At the transmitter, the N_T active feed antennas are connected to N_T dedicated RF chains, and the dual-functional signal is transmitted directly to a BD-RIS with N_I elements. The fully-connected BD-RIS considered in this work operates in the transmissive mode¹, where all N_I elements are connected to each other and allow incident signals to penetrate them only [7]. Moreover, BD-RIS is assumed to be deployed at a short distance, typically a few wavelengths away from the active antennas. The modeling of the channel matrix $\mathbf{H} \in \mathbb{C}^{N_I \times N_T}$ between the active antennas and the BD-RIS follows the uniform separate illumination (SI) strategy [2], [10]. And the scattering matrix of the fully-connected BD-RIS is a full matrix denoted by $\Psi \in \mathbb{C}^{N_I \times N_I}$. It satisfies the following symmetric and unitary constraint [6], [7]:

$$\Psi \in \mathcal{S}, \mathcal{S} = \{\Psi | \Psi = \Psi^T, \Psi^H \Psi = \mathbf{I}_{N_I}\}. \quad (1)$$

A dedicated low-cost sensor with N_S elements is placed at the BD-RIS to receive the echo signals from the three-hop link [12], i.e., the active antennas at the transmitter \rightarrow BD-RIS \rightarrow targets \rightarrow sensor. This reduces the number of hops and path loss as compared with the conventional receiver-side RIS-aided systems, where the sensing functionality is carried out at the transmitter far away from the RIS. Moreover, we assume that the side of the sensor facing the active antennas is physically blocked in order to achieve unidirectional reception of echo signals [12].

We consider M transmission blocks indexed by $\mathcal{M} = \{1, \dots, M\}$ in one coherent processing interval (CPI). The data streams for communication users at time index m are given as $\mathbf{c}[m] = [c_1[m], \dots, c_K[m]]^T \in \mathbb{C}^{K \times 1}$. $\mathbf{W} = [\mathbf{w}_1, \dots, \mathbf{w}_K] \in \mathbb{C}^{N_T \times K}$ denotes the corresponding digital precoding matrix. It remains consistent during one CPI. A dedicated sensing signal $\mathbf{s}_r[m] \in \mathbb{C}^{N_T \times 1}$ is considered in this work. Its covariance matrix is $\mathbf{R}_S = \mathbb{E}[\mathbf{s}_r[m]\mathbf{s}_r^H[m]]$. The transmit signal at time index m is given by

$$\mathbf{x}[m] = \mathbf{W}\mathbf{c}[m] + \mathbf{s}_r[m] = \sum_{k \in \mathcal{K}} \mathbf{w}_k c_k[m] + \mathbf{s}_r[m], \quad (2)$$

where the communication and sensing streams satisfy $\mathbb{E}[\mathbf{c}[m]\mathbf{c}^H[m]] = \mathbf{I}_K$, and $\mathbb{E}[\mathbf{c}[m]\mathbf{s}_r^H[m]] = \mathbf{0}_{K \times N_T}$, implying that the entries of the communication and sensing signals are independent from each other. The covariance matrix of the transmit signal is thereby given as $\mathbf{R}_X = \frac{1}{M} \sum_{m \in \mathcal{M}} \mathbf{x}[m]\mathbf{x}[m]^H = \mathbf{W}\mathbf{W}^H + \mathbf{R}_S$.

Communication users: The signal received at the communication user k at time index m is modeled as

$$y_k[m] = \mathbf{h}_k^H \Psi \mathbf{H} \mathbf{w}_k c_k[m] + \sum_{i \in \mathcal{K}, i \neq k} \mathbf{h}_k^H \Psi \mathbf{H} \mathbf{w}_i c_i[m] + \mathbf{h}_k^H \Psi \mathbf{H} \mathbf{s}_r[m] + z_k[m], \forall k \in \mathcal{K}, \quad (3)$$

¹We solely focus on the transmissive mode of BD-RIS. This choice is based on its demonstrated advantage of experiencing less feed blockage when positioned a few wavelengths away from the active antennas, as opposed to the reflective mode [2].

where $\mathbf{h}_k \in \mathbb{C}^{N_I \times 1}$ denotes the channel vector between the BD-RIS and user k , it is assumed to be perfectly known at the transmitter and user k . $z_k[m]$ is the additive white Gaussian noise (AWGN) with a distribution of $\mathcal{CN}(0, \sigma_c^2)$.

The signal to interference plus noise ratio (SINR) for decoding the desired signal of user k is given by

$$\gamma_k = \frac{|\mathbf{h}_k^H \Psi \mathbf{H} \mathbf{w}_k|^2}{\sum_{i \in \mathcal{K}, i \neq k} |\mathbf{h}_k^H \Psi \mathbf{H} \mathbf{w}_i|^2 + \mathbf{h}_k^H \Psi \mathbf{H} \mathbf{R}_S \mathbf{H} \Psi^H \mathbf{h}_k + \sigma_c^2}. \quad (4)$$

Therefore, the sum rate for communication users is calculated as $R_{\text{sum}} = \sum_{k=1}^K \log_2(1 + \gamma_k)$. This metric is selected to evaluate the communication performance in this work.

Sensing targets: The dual-functional signal $\mathbf{x}[m]$ is also exploited for target sensing. The received echo signal at the sensor from Q targets at time index m is given as

$$\mathbf{y}_r[m] = \mathbf{B} \mathbf{U} \mathbf{A}^T \Psi \mathbf{H} \mathbf{x}[m] + \mathbf{z}_r[m], \quad (5)$$

where

$$\begin{aligned} \boldsymbol{\alpha} &= [\alpha_1, \dots, \alpha_Q]^T, \mathbf{B} = [\mathbf{b}(\theta_1, \phi_1), \dots, \mathbf{b}(\theta_Q, \phi_Q)], \\ \mathbf{U} &= \text{diag}(\boldsymbol{\alpha}), \mathbf{A} = [\mathbf{a}(\theta_1, \phi_1), \dots, \mathbf{a}(\theta_Q, \phi_Q)], \end{aligned} \quad (6)$$

α_q in $\boldsymbol{\alpha}$ is a complex amplitude determined by the complex reflection coefficient and the path-loss of the q th target. θ_q and ϕ_q respectively denote the q th target's azimuth and elevation angle of departure (DoA) to the BD-RIS. $\mathbf{z}_r[m] \in \mathbb{C}^{N_S \times 1}$ is the AWGN following $\mathcal{CN}(\mathbf{0}_{N_S \times 1}, \sigma_r^2 \mathbf{I}_{N_S})$. Let $[\mathbf{r}_x, \mathbf{r}_y, \mathbf{r}_z] \in \mathbb{R}^{N_I \times 3}$ and $[\hat{\mathbf{r}}_x, \hat{\mathbf{r}}_y, \hat{\mathbf{r}}_z] \in \mathbb{R}^{N_S \times 3}$ respectively denote the Cartesian coordinates of the BD-RIS and the sensor. With the BD-RIS deployed in yz plane and the sensor along the y axis, i.e., $\mathbf{r}_x = \mathbf{0}$, $\hat{\mathbf{r}}_x = \hat{\mathbf{r}}_z = \mathbf{0}$, the steering vector can be calculated as $\mathbf{a}(\theta_q, \phi_q) = e^{-j \frac{2\pi}{\lambda} (\mathbf{r}_y \sin(\theta_q) \cos(\phi_q) + \mathbf{r}_z \sin(\phi_q))}$, and $\mathbf{b}(\theta_q, \phi_q) = e^{-j \frac{2\pi}{\lambda} (\hat{\mathbf{r}}_y \sin(\theta_q) \cos(\phi_q))}$, where λ denotes the wavelength of the carrier frequency.

The CRB matrix is exploited to measure the estimation performance. It is equivalent to the inverse of the fisher information matrix (FIM) \mathbf{F} [13]. $\mathbf{F} \in \mathbb{R}^{4Q \times 4Q}$ for estimating the parameter set $\xi_q = \{\theta_q, \phi_q, \text{Re}(\alpha_q), \text{Im}(\alpha_q)\}^T, \forall q \in \mathcal{Q}$ is

$$\mathbf{F} = \begin{bmatrix} \mathbf{F}_{\theta\theta} & \mathbf{F}_{\theta\phi} & \mathbf{F}_{\theta\text{Re}(\alpha)} & \mathbf{F}_{\theta\text{Im}(\alpha)} \\ \mathbf{F}_{\theta\phi}^T & \mathbf{F}_{\phi\phi} & \mathbf{F}_{\phi\text{Re}(\alpha)} & \mathbf{F}_{\phi\text{Im}(\alpha)} \\ \mathbf{F}_{\theta\text{Re}(\alpha)}^T & \mathbf{F}_{\phi\text{Re}(\alpha)}^T & \mathbf{F}_{\text{Re}(\alpha)\text{Re}(\alpha)} & \mathbf{F}_{\text{Re}(\alpha)\text{Im}(\alpha)} \\ \mathbf{F}_{\theta\text{Im}(\alpha)}^T & \mathbf{F}_{\phi\text{Im}(\alpha)}^T & \mathbf{F}_{\text{Re}(\alpha)\text{Im}(\alpha)}^T & \mathbf{F}_{\text{Im}(\alpha)\text{Im}(\alpha)} \end{bmatrix}, \quad (7)$$

where the entries of \mathbf{F} are derived in the Appendix A.

III. PROBLEM FORMULATION AND OPTIMIZATION FRAMEWORK

In this section, to enhance both the communication and sensing performance of the proposed BD-RIS-aided mmWave ISAC system model, we design the digital beamforming \mathbf{W} of the transmitter and the scattering matrix Ψ of the BD-RIS. Instead of proposing complex joint optimization methods for \mathbf{W} and Ψ , in this work, we propose a novel two-stage algorithm, where Ψ and \mathbf{W} are separately optimized as follows.

A. Stage 1: Proposed BD-RIS Scattering Matrix Design

Building upon the approach introduced in [14] for a BD-RIS-aided communication-only network, this subsection extends its application to an ISAC scenario where the BD-RIS scattering matrix is designed to jointly optimize the sum channel gains of the communication users and sensing targets. To obtain a feasible solution of the scattering matrix Ψ , we first relax the non-convex set \mathcal{S} in (1) to the set $\mathcal{M} = \{\Psi | \Psi^H \Psi = \mathbf{I}_{N_I}\}$, where $\mathcal{S} \in \mathcal{M}$. The relaxed problem to maximize the sum channel gains is formulated as

$$(\mathcal{P}_1) \max_{\Psi} f(\Psi) = \sum_{k=1}^K \|\mathbf{h}_k^H \Psi \mathbf{H}\|^2 + \|\mathbf{B}\mathbf{U}\mathbf{A}^T \Psi \mathbf{H}\|_F^2 \quad (8a)$$

$$s.t. \quad \Psi \in \mathcal{M}. \quad (8b)$$

The objective function can be further rewritten as $f(\Psi) = \|\mathbf{G}^H \Psi \mathbf{H}\|_F^2$, where $\mathbf{G} = [\mathbf{h}_1, \dots, \mathbf{h}_K, \mathbf{A}^* \mathbf{U}^H \mathbf{B}^H] \in \mathbb{C}^{N_I \times (K+N_S)}$. To derive the optimal solution of (8), we first define the singular value decomposition (SVD) of the matrix \mathbf{G}^H and \mathbf{H} as $\mathbf{G}^H = \mathbf{U}_1 \mathbf{S}_1 \mathbf{V}_1^H$ and $\mathbf{H} = \mathbf{U}_2 \mathbf{S}_2 \mathbf{V}_2^H$, where $\mathbf{U}_i, \mathbf{V}_i$ are unitary matrices while \mathbf{S}_i are diagonal matrices, $i = \{1, 2\}$.

Proposition 1. Define $\mathbf{X} = \mathbf{V}_1^H \Psi \mathbf{U}_2 \in \mathbb{C}^{N_I \times N_I}$, $\mathbf{\Sigma}_1 = \mathbf{S}_1^H \mathbf{S}_1 \in \mathbb{C}^{N_I \times N_I}$, and $\mathbf{\Sigma}_2 = \mathbf{S}_2 \mathbf{S}_2^H \in \mathbb{C}^{N_I \times N_I}$. Then, we obtain that $\text{Re}\{\text{tr}(\mathbf{\Sigma}_1 \mathbf{X} \mathbf{\Sigma}_2 \mathbf{X}^H)\} \leq \text{tr}(\mathbf{\Sigma}_1 \mathbf{\Sigma}_2)$, with equality holding if and only if $\mathbf{X} = \mathbf{I}_{N_I}$.

Proof: See Appendix B. \blacksquare

Based on Proposition 1, the objective function $f(\Psi)$ in (8a) becomes

$$f(\Psi) = \|\mathbf{U}_1 \mathbf{S}_1 \mathbf{V}_1^H \Psi \mathbf{U}_2 \mathbf{S}_2 \mathbf{V}_2^H\|_F^2$$

$$= \text{Re}\{\text{tr}(\mathbf{\Sigma}_1 \mathbf{X} \mathbf{\Sigma}_2 \mathbf{X}^H)\} \quad (9)$$

$$\leq \text{tr}(\mathbf{\Sigma}_1 \mathbf{\Sigma}_2),$$

where the equality holds if and only if $\mathbf{X} = \mathbf{I}_{N_I}$. Therefore, the optimal solution for the relaxed problem (8) is given by

$$\Psi^* = \mathbf{V}_1 \mathbf{U}_2^H. \quad (10)$$

Note that the optimal Ψ^* for problem (8) may not belong to the feasible set \mathcal{S} of the BD-RIS. The symmetric unitary projection proposed in [14] is then utilized to project a feasible solution on the set \mathcal{S} . Specifically, let $\tilde{\Psi} = \frac{\Psi^* + (\Psi^*)^T}{2}$, and suppose that it has a rank of g . Its SVD is $\tilde{\Psi} = \mathbf{U} \mathbf{S} \mathbf{V}^H$, where $\mathbf{U} = [\mathbf{U}_g \mathbf{U}_{N_I-g}]$ and $\mathbf{V} = [\mathbf{V}_g \mathbf{V}_{N_I-g}]$, respectively. A feasible scattering matrix Ψ on the set \mathcal{S} is then calculated as [14]

$$\Psi = \hat{\mathbf{U}} \mathbf{V}^H, \quad (11)$$

where $\hat{\mathbf{U}} = [\mathbf{U}_g, \mathbf{V}_{N_I-g}^*]$. (11) is known as the symmetric unitary projector which projects Ψ^* to \mathcal{S} .

B. Stage 2: Proposed Transmit Beamforming Design

With the scattering matrix Ψ obtained from (11), we then optimize the digital beamforming matrix \mathbf{W} with the aim of jointly maximizing the sum rate of the communication users and minimizing the largest eigenvalue of the CRB matrix of the sensing targets. Note that minimizing the largest eigenvalue

Algorithm 1: Beamforming optimization with BD-RIS

Stage 1: Design the scattering matrix Ψ .

Calculate the optimal Ψ^* on the relaxed set \mathcal{M} via (10).

Derive a feasible Ψ on the set \mathcal{S} via (11).

Stage 2: Design the transmit beamforming \mathbf{W} .

Initialize: $t \leftarrow 0$, $\{\mathbf{W}_{u,k}^{[t]}\}_{k=1}^K$, $\epsilon^{[t]}$, $\delta^{[t]}$, $\eta^{[t]}$;

repeat

Solve problem (18) with $\{\mathbf{W}_{u,k}^{[t]}\}_{k=1}^K$, $\epsilon^{[t]}$, $\delta^{[t]}$, $\eta^{[t]}$, and obtain the optimal $\{\mathbf{W}_{u,k}^*\}_{k=1}^K$, ϵ^* , δ^* , η^* and the optimal objective function value f_w^* ;

$t \leftarrow t + 1$;

Update $\{\mathbf{W}_{u,k}^{[t]}\}_{k=1}^K \leftarrow \{\mathbf{W}_{u,k}^*\}_{k=1}^K$, $\epsilon^{[t]} \leftarrow \epsilon^*$,

$\delta^{[t]} \leftarrow \delta^*$, $\eta^{[t]} \leftarrow \eta^*$, $f_w^{[t]} \leftarrow f_w^*$;

until $|f_w^{[t]} - f_w^{[t-1]}| < \epsilon$

of the CRB matrix of the sensing targets is equivalent to maximizing the smallest eigenvalue of \mathbf{F} [13]. By defining $\mathbf{W}_{u,k} = \mathbf{w}_k \mathbf{w}_k^H$, where $\text{rank}(\mathbf{W}_{u,k}) = 1, \forall k \in \mathcal{K}$ and introducing R_k as an auxiliary variable to denote the achievable rate of user k , $k \in \mathcal{K}$, the optimization problem is formulated as

$$(\mathcal{P}_2) \max_{\{\mathbf{w}_{u,k}\}_{k=1}^K, r, \mathbf{R}_X, \{R_k\}_{k=1}^K} \sum_{k=1}^K R_k + \mu r \quad (12a)$$

$$s.t. \quad \mathbf{F} \succeq r \mathbf{I}_{4Q}, \quad (12b)$$

$$\text{tr}(\mathbf{R}_X) \leq P, \quad (12c)$$

$$\mathbf{R}_X \succeq \sum_{k=1}^K \mathbf{W}_{u,k}, \quad \mathbf{W}_{u,k} \succeq \mathbf{0}, \forall k \in \mathcal{K}, \quad (12d)$$

$$\log_2 \left(1 + \frac{\mathbf{v}_k^H \mathbf{W}_{u,k} \mathbf{v}_k}{\mathbf{v}_k^H \mathbf{R}_X \mathbf{v}_k - \mathbf{v}_k^H \mathbf{W}_{u,k} \mathbf{v}_k + \sigma_c^2} \right) \geq R_k, \forall k \in \mathcal{K}, \quad (12e)$$

$$\text{rank}(\mathbf{W}_{u,k}) = 1, \forall k \in \mathcal{K}, \quad (12f)$$

where $\mathbf{v}_k^H = \mathbf{h}_k^H \Psi \mathbf{H}, \forall k \in \mathcal{K}$ represents the effective channel between the transmitter and user k . μ is a parameter used to shift the priority between the communication and sensing functionality. The matrix $(\mathbf{F} - r \mathbf{I}_{4Q})$ is guaranteed to be positive semi-definite by constraint (12b), where r corresponds to the smallest eigenvalue of \mathbf{F} . (12c) is the power constraint of the active antennas, with P denoting the total power budget. Note that the problem is non-convex owing to the rate expressions (12e) and the rank-one constraints (12f).

By introducing slack variables $\epsilon = [\epsilon_1, \dots, \epsilon_K]$ and $\delta = [\delta_1, \dots, \delta_K]$, we first rewrite (12e) as

$$\epsilon_k - \delta_k \geq R_k \ln 2, \forall k \in \mathcal{K}, \quad (13a)$$

$$e^{\epsilon_k} \leq \mathbf{v}_k^H \mathbf{R}_X \mathbf{v}_k + \sigma_c^2, \forall k \in \mathcal{K}, \quad (13b)$$

$$e^{\delta_k} \geq \mathbf{v}_k^H \mathbf{R}_X \mathbf{v}_k - \mathbf{v}_k^H \mathbf{W}_{u,k} \mathbf{v}_k + \sigma_c^2, \forall k \in \mathcal{K}. \quad (13c)$$

To deal with the non-convexity in (13c), we leverage the first-order Taylor approximation to approximate the left-hand

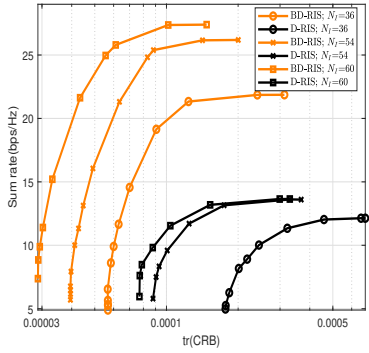


Fig. 2. The trade-offs under different numbers of BD-RIS elements. $K = 4$, $Q = 1$, $N_T = 6$, $N_S = 8$, $M = 128$, $P = 20$ dBm.

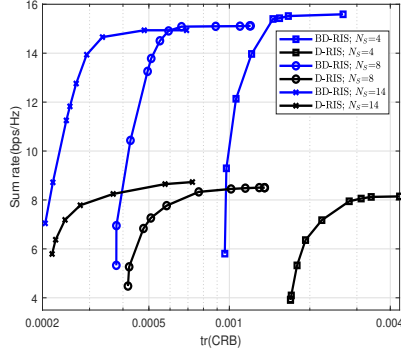


Fig. 3. The trade-offs under different numbers of sensor elements. $K = 4$, $Q = 1$, $N_I = 32$, $N_T = 4$, $M = 64$, $P = 15$ dBm.

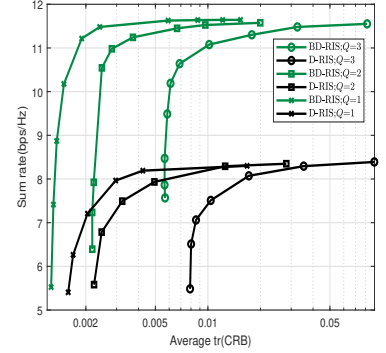


Fig. 4. The trade-offs under different numbers of targets. $K = 2$, $N_I = 16$, $N_T = 4$, $N_S = 4$, $M = 64$, $P = 20$ dBm.

side (LHS) of (13c) at the point $\delta_k^{[t]}$. (13c) is therefore approximated as

$$e^{\delta_k^{[t]}} (1 + \delta_k - \delta_k^{[t]}) \geq \mathbf{v}_k^H \mathbf{R}_X \mathbf{v}_k - \mathbf{v}_k^H \mathbf{W}_{u,k} \mathbf{v}_k + \sigma_c^2, \forall k \in \mathcal{K}, \quad (14)$$

where t denotes the t th SCA iteration. To achieve more efficient calculation via CVX, the slack variables $\boldsymbol{\eta} = [\eta_1, \dots, \eta_K]$ are further introduced to rewrite the non-linear terms e^{ϵ_k} , $\forall k \in \mathcal{K}$ in (13b), which is given by

$$\eta_k \leq \mathbf{v}_k^H \mathbf{R}_X \mathbf{v}_k + \sigma_c^2, \forall k \in \mathcal{K}, \quad (15a)$$

$$\eta_k \ln \eta_k \geq \eta_k \epsilon_k, \forall k \in \mathcal{K}. \quad (15b)$$

Similarly, $\eta_k \ln \eta_k$ on the LHS of (15b) is approximated at the point $\eta_k^{[t]}$, $\forall k \in \mathcal{K}$, and then transformed to its equivalent second-order cone (SOC) form as

$$\left\| \left[\eta_k + \epsilon_k - (1 + \ln \eta_k^{[t]}), 2\sqrt{\eta_k^{[t]}} \right] \right\|_2 \leq \eta_k - \epsilon_k + (1 + \ln \eta_k^{[t]}), \forall k \in \mathcal{K}. \quad (16)$$

With the normalized dominant eigenvector $\mathbf{p}_{k,max}^{[t]}$ of the matrix $\mathbf{W}_{u,k}^{[t]}$, $\forall k \in \mathcal{K}$, we then move the non-convex rank-one constraints (12f) to the objective function as

$$f_{\text{rank}} = \Gamma \sum_{k \in \mathcal{K}} \left(\text{tr}(\mathbf{W}_{u,k}) - (\mathbf{p}_{k,max}^{[t]})^H \mathbf{W}_{u,k} \mathbf{p}_{k,max}^{[t]} \right), \quad (17)$$

where Γ is a negative constant selected in order to guarantee that f_{rank} approaches zero closely.

Based on (13)–(17), problem (12) is approximated to a sequence of convex subproblems. Specifically, at iteration $t+1$, the following subproblem is tackled with $\mathbf{W}_{u,k}^{[t]}$, $\boldsymbol{\epsilon}^{[t]}$, $\boldsymbol{\delta}^{[t]}$, $\boldsymbol{\eta}^{[t]}$ obtained for the t th iteration:

$$(\mathcal{P}_3) \quad \max_{\{\mathbf{W}_{u,k}\}_{k=1}^K, \mathbf{R}_X, \{R_k\}_{k=1}^K, r, \boldsymbol{\epsilon}, \boldsymbol{\delta}, \boldsymbol{\eta}} \sum_{k=1}^K R_k + \mu r + f_{\text{rank}} \quad (18)$$

s.t. (12b)–(12d), (13a), (14), (15a), (16).

Problem (18) is convex, and it can be solved by CVX directly. We summarize the overall optimization process in Algorithm 1, where ε is the convergence tolerance.

IV. NUMERICAL RESULTS

In this section, we evaluate the performance of the proposed transmitter-side BD-RIS for mmWave ISAC. The sum rate $\sum_{k=1}^K R_k$ and the trace of the CRB are selected for evaluating communication and sensing performance, respectively. Note that when there are multiple sensing targets, the average $\text{tr}(\text{CRB})$ defined by $\text{tr}(\mathbf{F}^{-1})/Q$ is chosen to ensure comparison fairness. Unless otherwise specified, we consider $K = 4$ communication users and $Q = 1$ sensing target. We assume that the BD-RIS is 10 wavelengths away from the active antennas, with the carrier frequency set to $f_c = 30$ GHz. The communication users are randomly placed at $d_k = 30 \sim 50$ m away from the BD-RIS, where the communication channels \mathbf{h}_k are modeled as the Rician channels with the same parameter setting as in [12]. And we consider 3 different targets named target 1-3. They are located at $[d_q, \theta_q, \phi_q] = [30 \text{ m}, 30^\circ, 30^\circ]$, $[45 \text{ m}, 15^\circ, 60^\circ]$, and $[40 \text{ m}, 60^\circ, -45^\circ]$ with respect to the BD-RIS, respectively. The signal attenuation variance for sensing is calculated as $\sigma_{\alpha_q}^2 = \frac{\beta \lambda^2}{(4\pi)^3 d_q^4}$, where β denotes the radar cross section (RCS) and it is set to 5. The total power budget at the active antennas is $P = 20$ dBm, and the noise power is given as $\sigma_c^2 = -60$ dBm and $\sigma_r^2 = 0$ dBm [15]. Each CPI contains $N = 128$ transmission blocks.

To verify the efficiency of the transmitter-side BD-RIS-aided ISAC system, we select the conventional D-RIS-aided ISAC system as the baseline, where the D-RIS operates in the transmissive mode as well [10]. Let $\theta_{T,i}$, $i = [1, \dots, N_I]$ denote the phase shift angle of the conventional D-RIS. The corresponding diagonal scattering matrix $\boldsymbol{\Psi} = [e^{j\theta_{T,1}}, \dots, e^{j\theta_{T,N_I}}]$ can then be obtained via the same method as stated in [14]. The numerical results are obtained by averaging over 100 realizations.

In Fig. 2, we consider $N_T = 6$ active antennas and $N_S = 8$ sensor elements. We study the communication sum rate versus the sensing $\text{tr}(\text{CRB})$ for different numbers of BD-RIS elements N_I . As expected, better communication performance, i.e., the higher sum rate, as well as better sensing performance, i.e., the lower $\text{tr}(\text{CRB})$, are obtained with increasing BD-RIS elements. BD-RIS consistently achieves a better communication and sensing trade-off performance than the conventional D-RIS.

Moreover, the trade-off gain of BD-RIS over D-RIS is more explicit with increasing number of BD-RIS elements. This is attributed to the growing flexibility in BD-RIS design as the number of RIS elements increases.

In Fig. 3, we illustrate the influence of the number of the sensor elements N_S , where $N_I = 32$, $N_T = 4$, $M = 64$ and $P = 15$ dBm. It can be observed that as the number of sensor elements increases, the sensing performance becomes better, i.e., $\text{tr}(\text{CRB})$ becomes lower. Owing to the additional degree of freedom (DoF) introduced by the fully-connected passive elements to construct the directional sensing beam, BD-RIS dramatically enhances the sensing performance.

The trade-offs under different numbers of targets are demonstrated in Fig. 4, where $Q = 1$ (target 1), $Q = 2$ (target 1-2) and $Q = 3$ (target 1-3) are considered. There exists $K = 2$ communication users with $N_I = 16$, $N_T = 4$, $N_S = 4$ and $M = 64$. As observed, BD-RIS shows an explicit trade-off gain over the conventional D-RIS under different target numbers. The communication and sensing performance of both BD-RIS and the conventional D-RIS deteriorates as the number of targets increases. This is because less beamforming power is allocated to each sensing target. Surprisingly, BD-RIS shows the capability to detect more sensing targets than the conventional D-RIS while maintaining the same sum rate performance for communication users. This further shows the great potential of integrating BD-RIS into mmWave ISAC systems.

V. CONCLUSION

In this work, we propose a novel BD-RIS-aided transmitter architecture to reduce the power consumption and improve the communication and sensing performance for mmWave ISAC. The digital beamforming matrix of the transmitter and the scattering matrix of the BD-RIS are designed using the proposed two-stage algorithm with the aim of jointly maximizing the communication sum rate and minimizing the largest eigenvalue of the CRB matrix of the sensing targets. Numerical results demonstrate that the proposed transmitter-side BD-RIS significantly enhances the trade-off gain between communication and sensing compared to the conventional D-RIS. The results show the great potential of integrating BD-RIS into mmWave ISAC systems.

APPENDIX A

We define $\mathbf{u}_r[m] = \mathbf{y}_r[m] - \mathbf{z}_r[m] = \mathbf{B}\mathbf{U}\mathbf{A}^T\mathbf{\Psi}\mathbf{H}\mathbf{x}[m]$. With its partial derivative of $\text{Re}(\alpha_i)$, i.e., $\mathbf{B}\mathbf{e}_i\mathbf{e}_i^T\mathbf{A}^T\mathbf{\Psi}\mathbf{H}\mathbf{x}[m]$, $\forall i \in \mathcal{Q}$, the element of $\mathbf{F}_{\text{Re}(\alpha_i)\text{Re}(\alpha_j)} \in \mathbb{R}^{\mathcal{Q} \times \mathcal{Q}}$ in (7) is calculated as (see, e.g., [13, Appendix A])

$$\begin{aligned} \mathbf{F}_{\text{Re}(\alpha_i)\text{Re}(\alpha_j)} &= \frac{2}{\sigma_r^2} \text{Re} \left\{ \text{tr} \left\{ \sum_{m \in \mathcal{M}} \frac{\partial \mathbf{u}_r^H[m]}{\partial \text{Re}(\alpha_i)} \frac{\partial \mathbf{u}_r[m]}{\partial \text{Re}(\alpha_j)} \right\} \right\} \\ &= \frac{2M}{\sigma_r^2} \text{Re} \left\{ \mathbf{e}_j^T \mathbf{A}^T \mathbf{\Psi} \mathbf{H} \mathbf{R}_X \mathbf{H}^H \mathbf{\Psi}^H \mathbf{A}^* \mathbf{e}_i \mathbf{e}_i^T \mathbf{B}^H \mathbf{B} \mathbf{e}_j \right\} \\ &= \frac{2M}{\sigma_r^2} \text{Re} \left\{ (\mathbf{A}^H \mathbf{\Psi}^* \mathbf{H}^* \mathbf{R}_X^* \mathbf{H}^T \mathbf{\Psi}^T \mathbf{A})_{ij} (\mathbf{B}^H \mathbf{B})_{ij} \right\}, \forall i, j \in \mathcal{Q}, \end{aligned} \quad (19)$$

where $(\cdot)_{ij}$ denotes the element in the i th row and j th column. Other terms of FIM can be calculated in the same way, which are omitted here due to space limitation.

APPENDIX B

With $\mathbf{X} = \mathbf{V}_1^H \mathbf{\Psi} \mathbf{U}_2 \in \mathbb{C}^{N_I \times N_I}$, $\mathbf{\Sigma}_1 = \mathbf{S}_1^H \mathbf{S}_1 \in \mathbb{C}^{N_I \times N_I}$ and $\mathbf{\Sigma}_2 = \mathbf{S}_2 \mathbf{S}_2^H \in \mathbb{C}^{N_I \times N_I}$ defined in Section III-A, we have

$$\begin{aligned} \text{Re} \left\{ \text{tr} (\mathbf{\Sigma}_1 \mathbf{X} \mathbf{\Sigma}_2 \mathbf{X}^H) \right\} &= \sum_{i=1}^{N_I} \text{Re} \left\{ \text{tr} [\mathbf{\Sigma}_1 (\mathbf{\Sigma}_2)_{ii} \mathbf{x}_i \mathbf{x}_i^H] \right\} \\ &= \sum_{i=1}^{N_I} \sum_{j=1}^{N_I} (\mathbf{\Sigma}_1)_{jj} (\mathbf{\Sigma}_2)_{ii} |x_{ji}|^2 \leq \sum_{i=j=1}^{N_I} (\mathbf{\Sigma}_1)_{jj} (\mathbf{\Sigma}_2)_{ii}, \end{aligned} \quad (20)$$

where $\mathbf{x}_i = [x_{1i}, \dots, x_{N_I i}]^T \in \mathbb{C}^{N_I \times 1}$ denotes the i th column of the matrix \mathbf{X} . The inequality holds since $(\mathbf{\Sigma}_n)_{ii} \geq (\mathbf{\Sigma}_n)_{jj} \geq 0$, $i \leq j$, $n \in \{1, 2\}$, and $\mathbf{X} \in \mathcal{M}$. It is with equality if and only if $\mathbf{X} = \mathbf{I}_{N_I}$.

REFERENCES

- [1] F. Liu *et al.*, "Integrated sensing and communications: Toward dual-functional wireless networks for 6G and beyond," *IEEE J. Sel. Areas Commun.*, vol. 40, no. 6, pp. 1728–1767, 2022.
- [2] V. Jamali *et al.*, "Intelligent surface-aided transmitter architectures for millimeter-wave ultra massive MIMO systems," *IEEE Open J. Commun. Soc.*, vol. 2, pp. 144–167, 2021.
- [3] Z. Zhu *et al.*, "Resource allocation for IRS assisted mmWave integrated sensing and communication systems," in *Proc. IEEE Int. Conf. Commun. (ICC)*, 2022, pp. 2333–2338.
- [4] R. Li *et al.*, "Beam scanning for integrated sensing and communication in IRS-aided mmWave systems," in *Proc. IEEE Int. Workshop Signal Process. Adv. Wireless Commun. (SPAWC)*, 2023, pp. 196–200.
- [5] W. Lyu *et al.*, "CRB minimization for RIS-aided mmWave integrated sensing and communications," *IEEE Internet Things J.*, pp. 1–1, 2024.
- [6] S. Shen *et al.*, "Modeling and architecture design of reconfigurable intelligent surfaces using scattering parameter network analysis," *IEEE Trans. Wireless Commun.*, vol. 21, no. 2, pp. 1229–1243, 2022.
- [7] H. Li *et al.*, "Beyond diagonal reconfigurable intelligent surfaces: From transmitting and reflecting modes to single-, group-, and fully-connected architectures," *IEEE Trans. Wireless Commun.*, vol. 22, no. 4, pp. 2311–2324, 2022.
- [8] B. Wang *et al.*, "A dual-function radar-communication system empowered by beyond diagonal reconfigurable intelligent surface," *arXiv preprint arXiv:2301.03286*, 2023.
- [9] T. Esmailbeig *et al.*, "Beyond diagonal RIS: Key to next-generation integrated sensing and communications?" *arXiv preprint arXiv:2402.14157*, 2024.
- [10] W. Du *et al.*, "Hybrid beamforming design for ITS-assisted wireless networks," *IEEE Wireless Commun. Lett.*, vol. 12, no. 3, pp. 451–455, 2023.
- [11] A. Mishra *et al.*, "Transmitter side beyond-diagonal reconfigurable intelligent surface for massive MIMO networks," *IEEE Wireless Commun. Lett.*, vol. 13, no. 2, pp. 352–356, 2024.
- [12] Z. Wang *et al.*, "STARS enabled integrated sensing and communications," *IEEE Trans. Wireless Commun.*, vol. 22, no. 10, pp. 6750–6765, 2023.
- [13] J. Li *et al.*, "Range compression and waveform optimization for MIMO radar: A cramer-rao bound based study," *IEEE Trans. Signal Process.*, vol. 56, no. 1, pp. 218–232, 2008.
- [14] T. Fang *et al.*, "A low-complexity beamforming design for beyond-diagonal RIS aided multi-user networks," *IEEE Commun. Lett.*, vol. 28, no. 1, pp. 203–207, 2024.
- [15] J. Xiao *et al.*, "Efficient radar detection for RIS-aided dual-functional radar-communication system," in *Proc. IEEE 97th Veh. Technol. Conf. (VTC Spring)*, 2023, pp. 1–6.